 ISSN 0267-8179. DOI: 10.1002/jqs.3033

JQS Journal of Quaternary Science QRA Quaternary Research Association

Rapid Communication
The Laacher See Tephra discovered in southernmost Sweden

SIMON A. LARSSON* and STEFAN WASTEGÅRD
Department of Physical Geography, Stockholm University, Stockholm, Sweden

Received 7 February 2018; Revised 21 March 2018; Accepted 23 March 2018

ABSTRACT: We present the first geochemically confirmed finding of the Laacher See Tephra (LST) on the Swedish mainland, now the northernmost extension of the LST. Sediments were sampled at the Körslättamossen fen, southernmost Sweden, and a high-concentration cryptotephra occurrence (>65 000 shards cm^{-3}) of the LST was found in a sequence of calcareous gyttja. Tephra identification was confirmed by geochemical analysis using field-emission electron probe microanalysis and through comparison of the results with published LST data from proximal sites and distal sites north-east of Laacher See. The LST has previously been divided into eruption phases suggested to have spread in several dispersal fans, but it was not possible to confidently determine the phase of the tephra here closer than to the MLST or ULST. The finding of the LST presented here further strengthens the potential of tephrochronological studies in the south Scandinavian region.

KEYWORDS: EPMA; Laacher See Tephra; Lateglacial; Sweden; tephrochronology.

Introduction

The Laacher See Tephra (LST) originated from the explosive eruption of the Laacher See volcano in the East Eifel Volcanic Field in western Germany *c.* 12 900 cal a BP (Bronk Ramsey *et al.*, 2015). Through geochemical analysis of distal LST records and comparison with proximal LST geochemistry, the eruptive event has been reconstructed in detail and several phases have been identified, and the ashes of the distinct phases have been suggested to have dispersed in different directions (van den Bogaard and Schmincke, 1985; Harms and Schmincke, 2000). The phases are distinguished by different geochemical signatures of the tephras they produced, relating to the nature of the eruption during the individual phases, and were summarized by van den Bogaard and Schmincke (1985) as the LLST, the MLST–subdivided into A, B, C1, C2 and C3–and the ULST.

Three main dispersal fans were suggested by van den Bogaard and Schmincke (1985) and later built upon by, for example, Harms and Schmincke (2000) and Riede *et al.* (2011): a north-eastern fan consisting of the LLST, MLST B and MLST C1; a southern fan consisting of the MLST A, MLST C2 and ULST; and a south-western fan consisting only of the ULST (Fig. 1a). The MLST C3 phase was suggested to have spread east, but not reaching very far. The north-eastern fan appears to have spread the greatest distance from the eruption centre. The identification of the LLST and MLST C2 on the island of Bornholm is, until now, the most northerly geochemically confirmed record of the LST. A tentative identification of the LST was made in a marine core taken north-west of the island of Gotland in the Baltic Sea (Påhlsson and Bergh Alm, 1985). A few shards from that core were analysed by van den Bogaard and Schmincke (1985) and seem to correlate with the LST, although the results were only visualized in plots and the original data were not tabulated.

Here we present the discovery of the LST at a location in southernmost Sweden and briefly discuss its implications for the dispersal of the different eruption phases. It is the first geochemically confirmed occurrence of the LST in Sweden, as well as the most northerly confirmed LST finding to date.

*Correspondence: Simon A Larsson, as above.
E-mail: simon.larsson@natgeo.su.se

Study site

The Körslättamossen fen is located on the Söderåsen horst in north-west Scania, southernmost Sweden, some 740 km north-east of the Laacher See caldera (Fig. 1a). It is the remnant of a small, infilled and overgrown lake in a bedrock depression, and has a catchment area of *c.* 7.5 km^2 (Hammarlund and Lemdahl, 1994). The fen is covered partly by pasture land and partly by mixed spruce, pine and birch forest, within the latter of which the coring was performed in the central part of the fen (at 56°05′32.8″N, 13°03′50.0″E, Fig. 1b). The fen is situated at *c.* 118 m above sea level, which is about 70 m above the local marine limit (Fredén, 2009), and the area was deglaciated after *c.* 17 000 cal a BP (Stroeven *et al.*, 2016).

According to Hammarlund and Lemdahl (1994), the sediments of Körslättamossen consist of *c.* 1.8 m of fen peat underlain by >4 m of partly calcareous lake sediments from the Lateglacial–Early Holocene transition. Their chronology was based on radiocarbon dating and pollen analysis and implied a sedimentation onset sometime between 16 000 and 15 500 cal a BP as calibrated using OxCal Online (version 4.3), applying the IntCal13 calibration curve (Reimer *et al.*, 2013).

With the aim to correlate new results with those of Hammarlund and Lemdahl (1994), Körslättamossen was selected for tephra investigation and to test for the occurrence of the LST in southern Sweden. A report of the full tephra record of Körslättamossen is in preparation.

Methods

Coring was performed using a 7-cm-diameter, 70-cm-long Russian corer. Carbon content analysis and tephra extraction was performed on a core covering depths 250–320 cm beneath the surface.

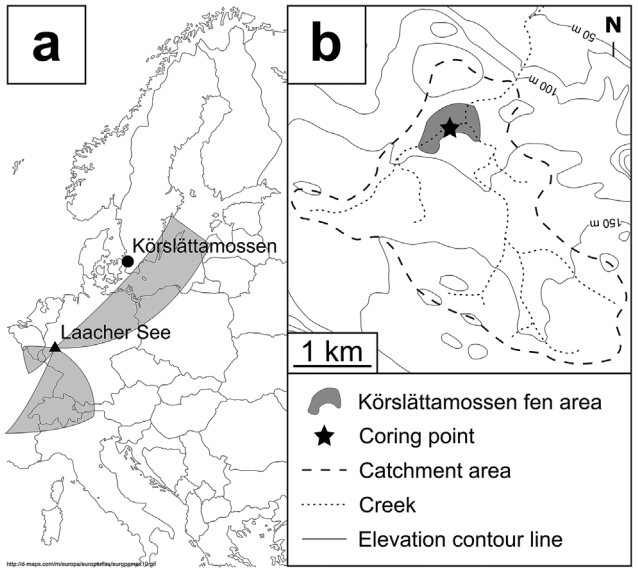

Figure 1. (a) Location of the study site, the Körslättamossen fen in southernmost Sweden and Laacher See in western Germany, as well as an approximation of the extent of the main dispersal fans as interpreted from Riede *et al.* (2011), where exact locations of previous LST finds are also presented. (b) Map of the Körslättamossen fen and its surroundings, and the location of the coring point.

Carbon content analysis was applied to samples at 2-cm resolution. Samples were prepared by drying at 105 °C overnight, grinding, re-drying and analysing *c.* 150–200 μm sample material at 550 °C and at 950 °C using an Eltra CS 500 Carbon–Sulfur Determinator. Results were interpreted as representative of organic carbon content when analysed at 550 °C and of inorganic carbon content at 950 °C.

Tephra extraction for microscopy followed Turney (1998), with some alterations: samples were (i) ashed at 550 °C for 3 h; (ii) dissolved in 10% hydrochloric acid overnight; (iii) sieved to retain material of grain sizes 25–100 μm; and (iv) centrifuged in sodium polytungstate to retain material of densities 2.3–2.5 g cm^{-3}. Remaining sample material was mounted on microscope slides using Canada balsam. The slides were searched for tephra using a light microscope equipped with a polarization filter.

The above was first applied on contiguous samples covering 5-cm depth each over the entire core and then repeated on samples covering 0.5-cm depth where tephra was found during the first microscopy search. For the second search, tablets of *Lycopodium* spores were added to the samples at the end of the extraction procedure. *Lycopodium* spores and tephra shards were counted during the second search to enable the estimation of tephra shard concentrations.

Tephra extraction for geochemical analysis was performed on a sample covering the 1.5-cm depth of highest estimated tephra concentration. The sample was put in a conical flask and boiled in 50 mL of 95% sulphuric acid while adding drops of 65% nitric acid until the colour of the fumes cleared. This was then diluted in water, then sieved and density-separated as in steps iii and iv above. The remaining sample material was mounted on frosted microscope slides using epoxy, which, after drying, was filed down to a thickness of *c.* 15 μm and subsequently polished and coated in carbon before chemical analysis by a JEOL JXA-8530F Hyperprobe field-emission electron probe microanalysis (FE-EPMA) device at Uppsala University, Sweden. MPI-DING glasses were analysed for calibration (Barker *et al.*, 2017) and compared to glass standards reported by Jochum *et al.* (2006). Calibration analysis results are available as Supporting Information (Table S1).

Results

The sediment of the investigated core was classified as relatively homogeneous, silty clay gyttja at 250–273 cm, calcareous gyttja with some clay, subtle laminations and abundant shell pieces at 273–296 cm, slightly laminated clay gyttja at 296–303 cm, underlain by another unit of calcareous gyttja at 303–320 cm (Fig. 2a,b). Organic carbon content varied between 1.2 and 7.3% and inorganic carbon content varied between 0.2 and 6.9% with higher values of both organic and inorganic carbon mainly in the calcareous gyttja units (Fig. 2c). The full carbon dataset is available in Table S2.

A high-concentration cryptotephra occurrence was found at 285–290-cm depth during the first tephra search. The second search resulted in an estimated maximum concentration of *c.* 65 500 shards cm^{-3} at 286–286.5 cm, with concentrations around 19 000 and 12 600 shards cm^{-3} in the 0.5 cm directly above and below, respectively (Fig. 2d). The tephra shards were highly vesicular (Fig. 3) and varied in size within the full sieved range, *i.e.* 25–100 μm. A separate tephra occurrence with a much lower concentration was found at 304–305-cm depth but was not geochemically analysed for this study.

Geochemical analysis was successfully performed on 21 shards (analyses that resulted in a major element weight percentage total <95 wt% were discarded). The average major element composition is presented in Table 1. The full geochemical analysis results are available in Table S3. The tephra had a phonolitic composition with 55.66–62.05 wt% SiO_2, 19.70–21.73 wt% Al_2O_3 and 5.87–7.45 wt % K_2O (Fig. 4).

Discussion

The visual appearance of the tephra shards found here is highly reminiscent of the more vesicular-type shards that have been described as occurring throughout the LST eruptive phases (van den Bogaard and Schmincke, 1985). Our results from the FE-EPMA are interpreted to confirm our identification of this tephra as the LST, after comparison with data of LST geochemistry from proximal sites (van den Bogaard and Schmincke, 1985; Harms and Schmincke, 2000) as well as distal sites located north-east of Laacher See (Turney *et al.*, 2006; Riede *et al.*, 2011; Housley *et al.*, 2013; Wulf *et al.*, 2013; Lane *et al.*, 2015; Jones *et al.*, 2018). Major element composition data from these studies were normalized to a 100% total for comparison purposes and are available in Table S4.

Visualizations of the geochemistry comparison are presented as major element bivariate plots in Fig. 4. The tephra found here is mostly separated from the LLST in terms of silica, titanium, magnesium and calcium content (which are mostly lower in the LLST), as well as sodium content (which is mostly higher in the LLST). It is, however, more difficult to identify this tephra as either one of the MLST or ULST phases, as most measurements place it as overlapping between the two. The combination of somewhat high silica and aluminium content may point to the MLST, while high iron and low sodium values may point to the ULST. We note, however, that sodium values are generally lower than in several other records from the north-eastern fan (e.g. Turney *et al.*, 2006; Housley *et al.*, 2013; Jones *et al.*, 2018). This issue has been recognized during previous geochemical analyses of distal LST (e.g. van den Bogaard and Schmincke, 1985; Wulf *et al.*, 2013), and could

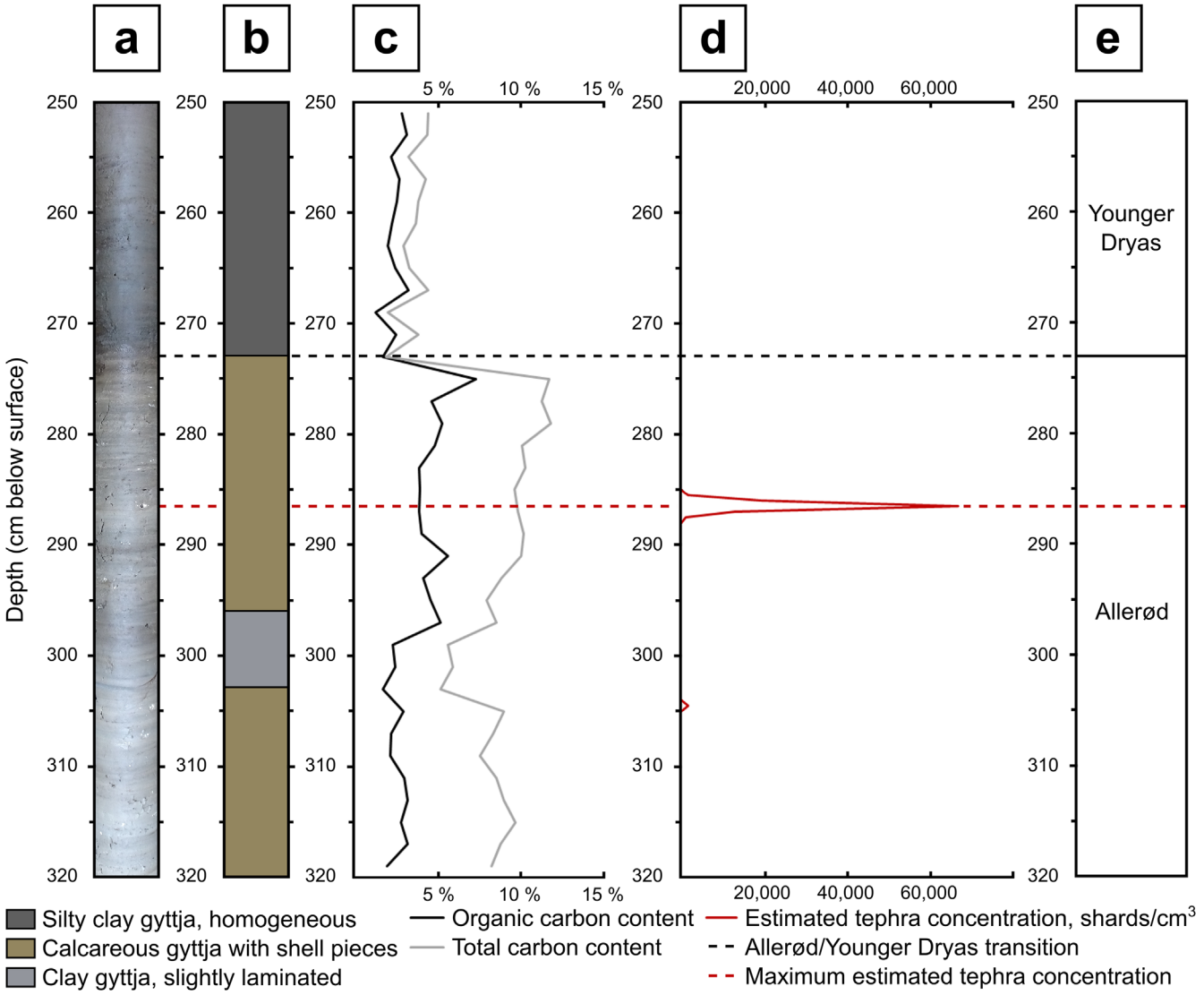

Figure 2. (a) Photograph of the core sampled at Körslättamossen, with (b) a simplified lithostratigraphic description, (c) organic and total carbon content, (d) estimated tephra concentrations of the 0.5-cm samples of the second tephra search, and (e) assumed chronostratigraphic units as per comparison with Hammarlund and Lemdahl (1994). Note that this figure only displays the one core discussed in this study, which only incorporates late Allerød and early Younger Dryas sediments.

be a result of sodium migration (see, for example, Gedeon *et al.*, 2000). The glass standard analyses for the EPMA equipment used here (Table S1) did not show any obvious sodium migration, which implies this may be a problem connected to distal LST, possibly due to the thinness of the vesicular-type tephra shards or an issue of glass alteration.

When compiling the data available from the several dozen sites where the LST had been found at the time, van den Bogaard and Schmincke (1985) suggested that the north-eastern dispersal fan consisted of the LLST, MLST B and MLST C1 eruptive phases, and that the MLST C2 and ULST phases exclusively spread to the south and south-west (or were at least 'strongly underrepresented' in the north-eastern dispersal fan). However, identification of the MLST C2 on Bornholm (Turney *et al.*, 2006), albeit somewhat uncertain, contradicts the suggestion that this phase only spread south. In much the same way, the possible identification of the ULST in south-west Poland (Housley *et al.*, 2013) contradicts that this phase, too, only spread south, and Jones *et al.* (2018) mention that their identification of possibly all three phases in northern Germany hints at a need for revision of the dispersal of the phases. Furthermore, Riede *et al.* (2011) argued that there is an overlap in the geochemistry of the MLST C and ULST phases – which

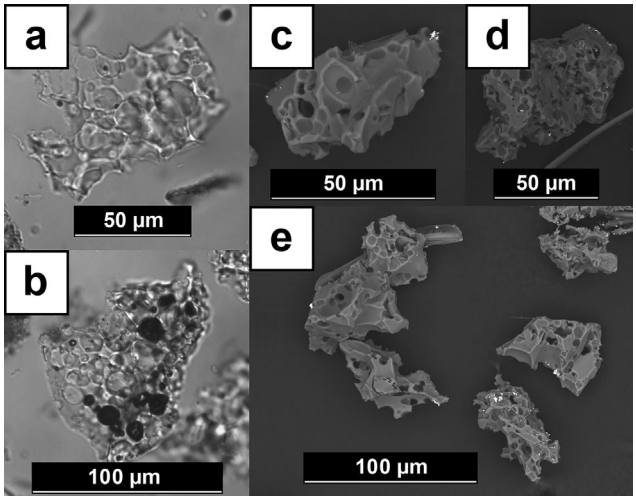

Figure 3. (a,b) Transmitted light and (c–e) scanning electron (SEM) micrographs of shards of the tephra found at Körslättamossen. SEM photos taken by Johan Lundberg at House of Science, Stockholm.

Table 1. Average major element composition of the tephra found at Körslättamossen, based on results from FE-EPMA performed on 21 tephra shards, presented as weight percentage and normalized to 100% total.

	SiO_2	TiO_2	Al_2O_3	FeO	MnO	MgO	CaO	Na_2O	K_2O	P_2O_5	Total
wt%	59.12	0.47	20.40	2.07	0.18	0.25	1.64	5.77	7.15	0.06	97.10
SD	1.35	0.05	0.50	0.19	0.05	0.05	0.35	0.58	0.37	0.04	1.75
norm. 100%	60.79	0.48	21.08	2.11	0.18	0.26	1.74	6.01	7.28	0.06	100
SD	0.77	0.05	0.42	0.20	0.05	0.05	0.36	0.56	0.38	0.04	0.00

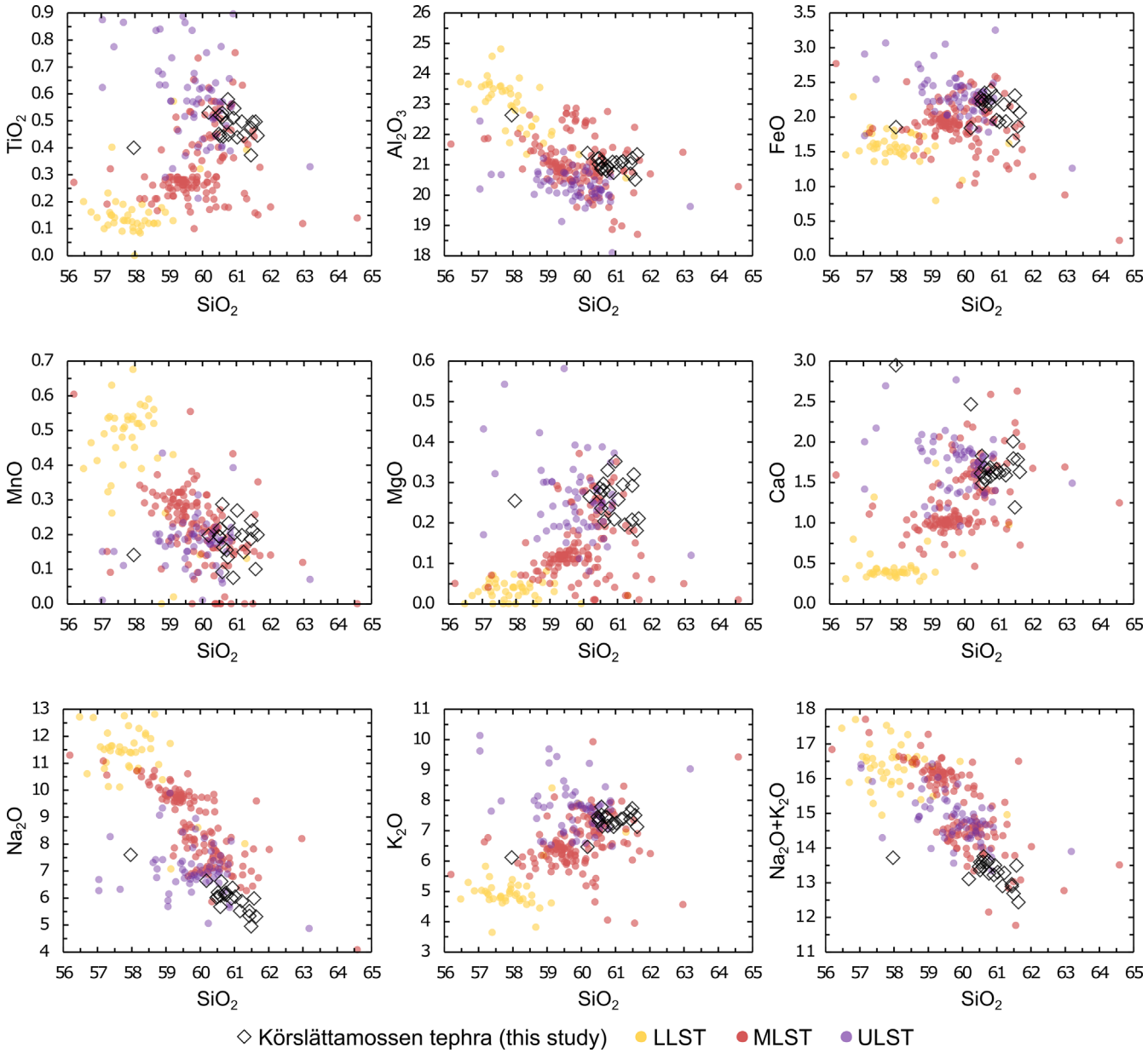

Figure 4. Bivariate plots of major elements displaying results from FE-EPMA of the tephra found at Körslättamossen and the corresponding ranges of the LLST, MLST and ULST in selected published literature. All data are normalized to a 100% total. Data used for the LLST, MLST and ULST are from: van den Bogaard and Schmincke (1985), Harms and Schmincke (2000), Turney *et al.* (2006), Riede *et al.* (2011), Housley *et al.* (2013), Wulf *et al.* (2013), Lane *et al.* (2015) and Jones *et al.* (2018).

was also noticed by Turney *et al.* (2006) – as well as the MLST A and MLST B phases, complicating phase identifications of the LST. It could be argued that the LST in Körslättamossen is in the mentioned overlap between the MLST and ULST. Similarly, Wulf *et al.* (2013) claimed to have found the MLST C and/or ULST in northern Poland, and were unable to distinguish between them. We cannot confidently determine which phase the LST in Körslättamossen belongs to, and we stress that there are issues regarding the LST phases and their dispersal that have yet to be resolved.

Conclusions

The discovery of the LST at Körslättamossen in southernmost Sweden reveals this tephra's dispersal to the north-east further north than previously confirmed, and possibly expands the

north-eastern dispersal fan slightly further west. This record of the LST strengthens the potential of tephrochronology in the south Scandinavian region by extending a Central European tephra to southern Sweden, thereby increasing the overlap and connections between the European and Icelandic tephra frameworks, as envisioned by, for example, Turney *et al.* (2006) after finding the LST on Bornholm. Future tephrochronological work in this region should exploit the possibility of finding the LST in new locations.

Acknowledgements. This project was funded by the Swedish Research Council (grant no. 2015-05255 to Stefan Wastegård). The authors would like to thank Dan Hammarlund at Lund University for directing us to the field site, Helene Sunmark for her aid during the fieldwork, Abigail Barker at Uppsala University for her aid during the microprobe session, Charlotte Flodin and Johan Lundberg at House of Science for arranging the electron microscopy session, as well as Felix Riede at Aarhus University for sharing the LST supplement to Tephrabase.

Supporting information

Table S1. FE-EPMA secondary glass standards analysed in connection with the analyses of the tephra found in this study (Barker *et al.*, 2017). Glass from Max Planck Institute (MPI-DING) with preferred values from Jochum *et al.* (2006). Only analyses comprising > 95 wt% are shown.

Table S2. Carbon content analysis results of 35 samples combusted at 550 °C (organic carbon content) and at 950 °C (inorganic carbon content), as well as the total carbon content.

Table S3. Geochemical analysis results from the FE-EPMA session at Uppsala University: major element composition of the tephra found in this study expressed as normalized weight percentage as well as normalized to 100% total.

Table S4. Selected published LST geochemistry data normalized to 100% total for comparison purposes. Note references for original publications.

Abbreviations. BP, before present (i.e. before 1950 CE); FE-EPMA, field-emission electron probe microanalysis; LST, Laacher See Tephra; LLST, Lower Laacher See Tephra; MLST, Middle Laacher See Tephra; MPI-DING, Max-Planck-Institut–Dingwell; ULST, Upper Laacher See Tephra.

References

Barker AK, Muir DD, Majka JM *et al.* 2017. Precision and accuracy of glass analyses by EMP at Uppsala University. *Earth Chemical Library*. DOI 10.1594/IEDA/100696.

Bronk Ramsey C, Albert PG, Blockley SPE *et al.* 2015. Improved age estimates for key Late Quaternary European tephra horizons in the RESET lattice. *Quaternary Science Reviews* **118**: 18–32.

Fredén C, ed. 2009. *Sveriges Nationalatlas: Berg och jord*. Gävle, Sweden: Kartförlaget.

Gedeon O, Hulínský V, Jurek K. 2000. Microanalysis of glass containing alkali ions. *Microchimica Acta* **132**: 505–510.

Hammarlund D, Lemdahl G. 1994. A Late Weichselian stable isotope stratigraphy compared with biostratigraphical data: a case study from southern Sweden. *Journal of Quaternary Science* **9**: 13–31.

Harms E, Schmincke H-U. 2000. Volatile composition of the phonolitic Laacher See magma (12,900 yr BP): implications for syn-eruptive degassing of S, F, Cl and H_2O. *Contributions to Mineralogy and Petrology* **138**: 84–98.

Housley RA, MacLeod A, Nalepka D *et al.* 2013. Tephrostratigraphy of a Lateglacial lake sediment sequence at Wegliny, southwest Poland. *Quaternary Science Reviews* **77**: 4–18.

Jochum KP, Stoll B, Herwig K *et al.* 2006. MPI-DING reference glasses for in situ microanalysis: New reference values for element concentrations and isotope ratios. *Geochemistry Geophysics Geosystems* **7**: Q02008.

Jones G, Lane CS, Brauer A *et al.* 2018. The Lateglacial to Early Holocene tephrochronological record from Lake Hämelsee, Germany: a key site within the European tephra framework. *Boreas* **47**: 28–40.

Lane CS, Brauer A, Martín-Puertas C *et al.* 2015. The Late Quaternary tephrostratigraphy of annually laminated sediments from Meerfelder Maar, Germany. *Quaternary Science Reviews* **122**: 192–206.

Påhlsson I, Bergh Alm K. 1985. Pollen-analytical studies of the cores 14103-3 and 14102-1 from the western Baltic. *Striae* **23**: 74–82.

Reimer PJ, Bard E, Bayliss A *et al.* 2013. IntCal13 and Marine13 radiocarbon age calibration curves 0–50, 000 years cal BP. *Radiocarbon* **55**: 1869–1887.

Riede F, Bazely O, Newton AJ *et al.* 2011. A Laacher See-eruption supplement to Tephrabase: investigating distal tephra fallout dynamics. *Quaternary International* **246**: 134–144.

Stroeven AP, Hättestrand C, Kleman J *et al.* 2016. Deglaciation of Fennoscandia. *Quaternary Science Reviews* **147**: 91–121

Turney CSM. 1998. Extraction of rhyolitic component of Vedde microtephra from minerogenic lake sediments. *Journal of Paleolimnology* **19**: 199–206.

Turney CSM, Den Burg KV, Wastegård S *et al.* 2006. North European last glacial–interglacial transition (LGIT; 15–9 ka) tephrochronology: extended limits and new events. *Journal of Quaternary Science* **21**: 335–345.

van den Bogaard P, Schmincke H-U. 1985. Laacher See Tephra: a widespread isochronous late Quaternary tephra layer in central and northern Europe. *Geological Society of America Bulletin* **96**: 1554–1571.

Wulf S, Ott F, Słowiński M *et al.* 2013. Tracing the Laacher See Tephra in the varved sediment record of the Trzechowskie palaeolake in central Northern Poland. *Quaternary Science Reviews* **76**: 129–139.

